Thermochimica Acta, 186 (1991) 153–169
Elsevier Science Publishers B.V., Amsterdam

The kinetic analysis of the crystallization processes in glasses

Jiří Málek and Vít Smrčka

Joint Laboratory of Solid State Chemistry of the Czechoslovak Academy of Sciences and Institute of Chemical Technology, Cs. Legii sq. 512, Pardubice 532 10 (Czechoslovakia)

(Received 21 December 1990)

Abstract

The crystallization kinetics characterized under non-isothermal conditions using thermal analysis (TA) techniques are discussed.

A simple and consistent method of kinetic analysis of TA data has been developed. The method allows one to perform the correct determination of the most suitable kinetic model and subsequent calculation of all kinetic parameters needed for a quantitative description of the studied process. This method was used to study the kinetics of crystallization of $(GeS_2)_{0.3}(Sb_2S_3)_{0.7}$ glass measured by various DSC and DTA instruments. The influence of instrumental factors is discussed with respect to the reliability of the kinetic information deduced from the experimental data.

INTRODUCTION

The crystallization processes in glasses have received a great deal of attention in the last two decades [1–5]. Kinetic investigations of these processes are of interest for elucidating the nature of crystal growth and for research on glass ceramic materials. Although the general theory of transformation kinetics is largely confined to the description of the isothermal transformation condition, there are many instances where the kinetic behavior of a system which is heated or cooled through the transformation region is of greater practical importance.

Non-isothermal experiments can be used to extend the temperature range of measurements beyond that accessible to isothermal experiments. Many crystallization processes occur too rapidly to be measured under isothermal conditions because of transients inherently associated with the instrument. In this respect a study of crystallization kinetics under non-isothermal conditions is desirable.

Differential scanning calorimetry (DSC) and quantitative differential thermal analysis (DTA) are widely used techniques for obtaining kinetic information about the crystallization processes. The vast majority of instruments available commercially are capable of producing reliable and accurate data. Nevertheless, there is still an open question: how to determine cor-

0040-6031/91/$03.50

rectly the kinetic parameters and how these parameters are affected by the instrumental factors and experimental conditions.

We therefore decided to develop a method allowing reliable kinetic analysis and interpretation of DSC and DTA data. This method was applied to perform a kinetic analysis of crystallization of chalcogenide glass measured by various DSC and DTA instruments. A computer program has been written enabling the calculations required. The results are compared and discussed with respect to the reliability of the kinetic analysis.

THEORY

The kinetic equation

The experimental DSC or DTA data are usually obtained in the form of data pairs T_i, $\dot{H}_i$, where T_i is the temperature of the studied system and $\dot{H}_i$ is the measured heat flow (DSC) or proportional quantity (quantitative DTA) at a heating rate β. Starting from these data we can calculate the degree of conversion α_i using the equation

$$\alpha_i = \frac{1}{\beta \Delta H_e} \int_{T_1}^{T_i} \dot{H} \, dT \tag{1}$$

where T_1 is the temperature at the beginning of a DSC or DTA peak and ΔH_e is the measured reaction heat, determined by integration of the crystallization peak area. We have, therefore, the following sequence of kinetic data: T_1, $\dot{H}_1$, $\alpha_1 \ldots T_i$, $\dot{H}_i$, $\alpha_i \ldots T_n$, $\dot{H}_n$, α_n where n is the number of data points.

The mathematical expression for the kinetic equation can be written as

$$\dot{H} = \Delta H_c A \, e^{-x} f(\alpha) \tag{2}$$

where ΔH_c is the calculated reaction heat and $x = E/RT$. The function $f(\alpha)$ in eqn. (2) is an analytical expression describing the kinetic model of the studied process. The most frequently used $f(\alpha)$ functions [6] are sum-

TABLE 1

The kinetic models

Model	Symbol	$f(\alpha)$
Šesták–Berggren eqn.	SB(m, n)	$\alpha^m(1-\alpha)^n$
Johnson–Mehl–Avrami eqn.	JMA(n)	$n(1-\alpha)[-\ln(1-\alpha)]^{1-1/n}$
Reaction order eqn.	RO(n)	$(1-\alpha)^n$
Two-dimensional diffusion	D2	$1/[-\ln(1-\alpha)]$
Jander eqn.	D3	$3(1-\alpha)^{2/3}/2[1-(1-\alpha)^{2/3}]$
Ginstling–Brounshtein eqn.	D4	$\frac{3}{2}[(1-\alpha)^{-1/3}-1]$

marized in Table 1. The parameters A and E as well as the exponent n (or m) of the $f(\alpha)$ function are characteristic constants.

If the temperature rises at a constant rate β, then we obtain after integration of eqn. (2) the equation

$$g(\alpha) = \int_0^{\alpha} \frac{d\alpha}{f(\alpha)} = \frac{AE}{\beta R} e^{-x}\left[\frac{\pi(x)}{x}\right] \tag{3}$$

where $\pi(x)$ is an approximation of the temperature integral [6]. There are many approximate expressions of the $\pi(x)$ function in the literature. According to our experience, the rational expression of Senum and Yang [7] is sufficient because it gives errors lower than $10^{-5}\%$ for $x > 20$

$$\pi(x) = \frac{x^3 + 18x^2 + 88x + 96}{x^4 + 20x^3 + 120x^2 + 240x + 120}$$

Calculation of E

There are many methods to calculate the activation energy from kinetic data. As is shown below, this parameter can hardly be ascertained by analyzing the kinetic data taken only at one heating rate. This is because of the strong mutual interdependence of parameters E and A in eqn. (2). Hence it is more suitable to apply so called multiple scan methods using several sets of kinetic data taken at various heating rates.

Probably the most popular in this family is the Kissinger method [8], where the activation energy is calculated using a plot of $\ln(\beta/T_p^2)$ versus $1/T_p$, the slope of which is $-E/R$. Another calculation method was introduced by Ozawa [9] and is based on a plot of $\ln(\beta)$ versus $1/T_p$, with slope $-1.052\ E/R$. The parameter T_p is the temperature of the maximum of the DSC or DTA peak.

An alternative method is known as the Friedman [10] (or isoconversional) plot, i.e. $\ln \dot{H}_\alpha$ versus $1/T_\alpha$, which gives the slope $-E/R$ at a constant degree of conversion α. The linearity of the slope for several values of α is a test of the constancy of E with respect to the degree of conversion.

Determination of the kinetic model

By combining eqns. (2) and (3) we can obtain [11]

$$z(\alpha) = T\dot{H}\pi(x)/\beta = \Delta H_c f(\alpha) g(\alpha) \tag{4}$$

If the activation energy is known, the $z(\alpha) = T\dot{H}\pi(x)/\beta$ curve can be calculated from kinetic data. This curve has a maximum at α_p^{∞} for which a general condition exists in the form [11]

$$-f'(\alpha_p^{\infty}) g(\alpha_p^{\infty}) = 1 \tag{5}$$

It should be pointed out that the value of α_p^∞ also corresponds to the maximum of a hypothetical DSC or DTA peak for $x_p \to \infty$. This parameter has a characteristic value [11] for the D2, D3, D4 and JMA(n) models as summarized in Table 2. It is interesting that α_p^∞ is practically independent of the activation energy (in fact it varies within 1% of the theoretical value). For the SB(m, n) and the RO(n) model α_p^∞ depends on the value of the kinetic exponent n or m.

By rewriting eqn. (2) in a somewhat different form we obtain

$$y(\alpha) = \dot{H}\, e^x = A' f(\alpha) \tag{6}$$

where $A' = \Delta H_c A$, which is a constant. Thus by plotting the $y(\alpha)$ dependence, normalized within the $\langle 0, 1 \rangle$ interval, the shape of $f(\alpha)$ is obtained. It is clear that the shape of the $f(\alpha)$ function is characteristic for each kinetic model. From this point of view the following rules can be formulated:

(i) If the $y(\alpha)$ function decreases steadily it has a maximum at $\alpha_m = 0$. This function can be convex [$y(\alpha_i) > \alpha_i$], linear [$y(\alpha_i) = \alpha_i$] or concave [$y(\alpha_i) < \alpha_i$]. Convex dependence corresponds to the RO($n < 1$) model, linear dependence to the JMA(n) model and concave dependence to the D2, D3, D4 or RO($n > 1$) model.

(ii) If there is a maximum of the $y(\alpha)$ function at $\alpha_m \in (0, 1)$ the kinetic data can be described by the SB(m, n) or JMA($n > 1$) model.

Both the $y(\alpha)$ and $z(\alpha)$ dependences can be used to guide the choice of a kinetic model [11,12]. The α_m and α_p^∞ values are especially useful in this respect. Their combination allows the determination of the most suitable kinetic model as shown by the scheme in Fig. 1.

In contrast to the α_p^∞ parameter, α_m is strongly affected by E. Hence the activation energy is decisive for a reliable determination of the kinetic model because, by varying E, a particular set of kinetic data can be interpreted within the scope of several kinetic models. From this point of view the SB(m, n) model can be considered as a general one because all other models [i.e. JMA(n), D2, D3 and D4] can be expressed by means of it. Of course, this is not true for a fixed value of the activation energy [13]. It should be pointed out that the kinetic exponents m and n are interdependent, as

TABLE 2

The characteristic values of parameter α_p^∞

Model	α_p^∞
JMA(n)	0.633
D2	0.834
D3	0.704
D4	0.776

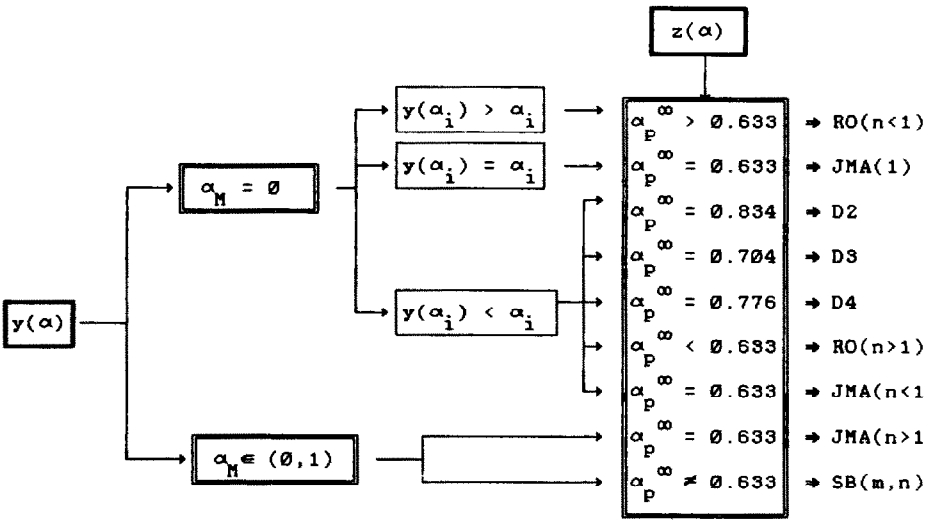

Fig. 1. Schematic diagram of the kinetic model determination.

shown in Fig. 2. The values of these exponents within acceptable limits [a] are defined by parameter α_m (broken lines), which depends on the activation energy. This "effective" activation energy E' is defined by the relation: $E' < rE$, where r is a constant. Thus constant r can be calculated by the Freeman and Carroll method [15,16] as the RO(n') model equivalent to the true kinetic model (i.e. $r = E'/E$). The parameters r and n' are shown in Table 3. These parameters differ slightly from the values reported by Criado et al. [16]. The deviation can be explained by the different types of $\pi(x)$ function used for the calculation.

Seeing that the kinetic model varies with the effective activation energy in this way, it can hardly be fruitful to try to analyze the kinetic data unless the value of E is known a priori. Therefore, for a reliable analysis of the kinetic data, first of all we have to calculate the value of the activation energy. Then we are able to determine the kinetic model using the method described above.

Calculation of kinetic exponents

Once the kinetic model has been determined, the kinetic exponents n (or m) can be calculated for the RO(n), JMA(n) or SB(m, n) model. The calculation methods depend on the particular kinetic model and are described below.

[a] Recently it was shown [14] that the parameter m should be lower than unity.

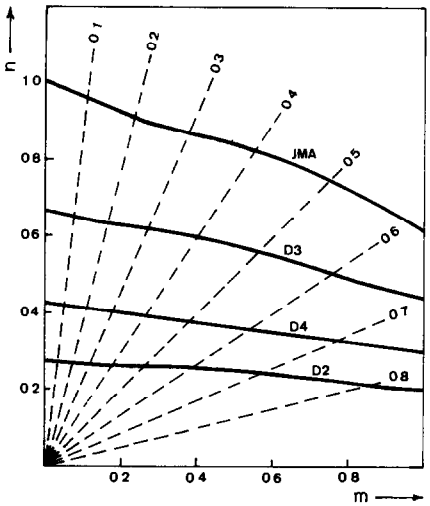

Fig. 2. The combinations of kinetic exponents of the SB(m, n) model corresponding to the D2, D3, D4 and JMA(n) models (full lines). The values of α_m are shown by the broken lines.

RO(n) *model*

The kinetic exponent for this model can be calculated iteratively using the equation

$$\alpha_p = 1 - \left[1 + \frac{1-n}{n} x_p \pi(x_p)\right]^{1/(n-1)} \qquad n \neq 1 \tag{7}$$

where α_p and x_p correspond to the maximum of the DSC peak. This equation was derived originally by Gorbachev [17] for $\pi(x) = 1/(x_p + 2)$.

JMA(n) *model*

If the $y(\alpha)$ function has a maximum at α_m (i.e. $n > 1$) the kinetic exponent n can be calculated using the equation [12]

$$n = \frac{1}{1 + \ln(1 - \alpha_m)} \tag{8}$$

If there is no maximum of the $y(\alpha)$ function, the parameter n can be calculated by means of the Šatava method [18], i.e. from the slope of the plot

TABLE 3

The values of parameters r and n'

Model	n'	r
JMA(n)	1	$1.07n - 0.07$
D2	0.303	0.469
D3	0.667	0.471
D4	0.434	0.465

of $\ln[-\ln(1-\alpha)]$ vs. $1/T$, which is nE/R. An alternative method of calculation is based on the relation derived from the condition for the maximum of the DSC peak [19]

$$n = \frac{1 - x_p \pi(x_p)}{\ln(1-\alpha_p) + 1} \tag{9}$$

It is known that the Šatava method gives slightly higher values of the parameter n. On the other hand, eqn. (9) gives a lower value. From our experience it seems that an average of these two values is a good approximation of the kinetic exponent.

SB(m, n) *model*

The kinetic parameter ratio $p = m/n$ can be calculated using the equation [12]

$$p = \frac{\alpha_m}{1 - \alpha_m} \tag{10}$$

Then eqn. (2) may be expressed in the form

$$\ln(\dot{H}\, e^x) = \ln(\Delta H_c A) + n \ln[\alpha^p (1-\alpha)] \tag{11}$$

The kinetic parameter n corresponds to the slope of linear dependence of $\ln(\dot{H}\, e^x)$ vs. $\ln[\alpha^p(1-\alpha)]$ for $\alpha \in (0.2, 0.8)$. Then the second kinetic exponent is $m = pn$.

Calculation of A *and* ΔH_c

Knowing the value of the activation energy and the kinetic exponent, the preexponential factor can be calculated using the equation [12]

$$A = -\frac{\beta x_p}{T_p f'(\alpha_p)} \exp(x_p) \tag{12}$$

The reaction heat ΔH_c is then expressed by

$$\Delta H_c = \frac{1}{A} \sum_{i=1}^{n} \frac{\dot{H}_i \exp(x_i)}{f(\alpha_i)} \tag{13}$$

KINETIC PROGRAM

Figure 3 is a simple schematic representation of the overall kinetic software package written for an IBM or compatible PC-AT computer. The program DATAPRO transforms raw DSC data (T_i, H_i) into the kinetic data (T_i, α_i, H_i) using eqn. (1). Then there are three programs FRIEDMAN, OZAWA and KISSINGER, to calculate the activation energy from several sets of kinetic

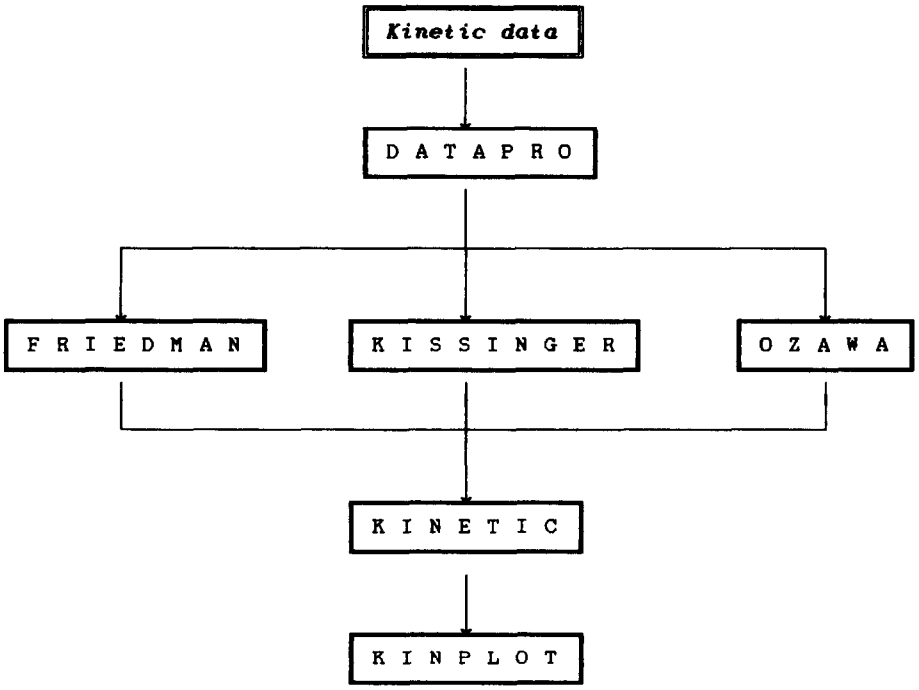

Fig. 3. Schematic diagram of the kinetic program.

data at various heating rates. These values are used by the program KINETIC to calculate both $y(\alpha)$ and $z(\alpha)$ functions normalized to the interval $\langle 0, 1 \rangle$ for a particular kinetic dataset. The maxima of these functions enables the proposal of the most suitable kinetic model (see Fig. 1). Once the kinetic model is known, the remaining kinetic parameters are calculated using eqns. (7)–(13). Both experimental and calculated DSC and DTA curves for several heating rates are plotted by the program KINPLOT.

EXPERIMENTAL

The studied glass, of composition $(GeS_2)_{0.3}(Sb_2S_3)_{0.7}$, was prepared using germanium, antimony and sulfur with nominal purity 5N. A mixture of these elements was placed in a quartz ampoule which was then evacuated to a pressure of 10^{-4} Pa and sealed. After heat treatment (10 h, 900 °C), the ampoule was rapidly cooled in water to room temperature. The glassy nature of the sample was confirmed by X-ray diffraction analysis. The primary $(GeS_2)_{0.3}(Sb_2S_3)_{0.7}$ was crushed into a powder and then sieved to particle size $70 < z < 90$ μm. This powder was used for the crystallization kinetics measurements.

The crystallization kinetics of glassy $(GeS_2)_{0.3}(Sb_2S_3)_{0.7}$ were studied in a series of non-isothermal experiments performed with five different instru-

TABLE 4

Instruments and temperature ranges (ΔT) used for the measurements

Symbol	Instrument	Data acquisition	ΔT (K)
A	Perkin–Elmer DSC-7	PE-7700/TAS	523–723
B	Perkin–Elmer DSC-4	PE-3600/TADS	383–723
C	Perkin–Elmer DTA-1700 [a]	PE-3600/TADS	298–900
D	DuPont-990	chart recorder	473–803
E	Perkin–Elmer DSC-2	digital output	454–700

[a] Measurements were carried out in the DSC mode [20].

ments as summarized in Table 4. The first three instruments (*A*, *B* and *C*) were coupled with a data acquisition system (TAS or TADS) supplied by the Perkin–Elmer Corporation and the other two had analog and digital output. Temperature and caloric calibrations were performed for each instrument at all heating rates using high purity Pb and Zn standards. Linear baseline interpolation was used for the integration of crystallization peaks.

All experiments were carried out on samples of about 10 mg in sealed Al pans, with an empty pan as the standard. The measurements were performed at four different heating rates, i.e. 2 (2.5), 5, 10 and 20 K min^{-1}, in the temperature interval (ΔT) shown in Table 4. Except for instrument *A*, all measurements were started well below the glass transition temperature ($T_g = 517$ K at $\beta = 10$ K min^{-1}). There was observed one well defined crystallization peak in the temperature region 590–680 K corresponding to the crystallization of the Sb_2S_3, phase as was confirmed by X-ray diffraction analysis.

RESULTS AND DISCUSSION

Figure 4 shows both experimental (points) and calculated crystallization peaks of $(GeS_2)_{0.3}(Sb_2S_3)_{0.7}$ glass obtained by instruments *A* and *C*. This is a typical output of the kinetic program described in Section 3. By analyzing these curves the activation energy can be determined using the methods described above. The values of *E* determined by the Friedman method are shown in Fig. 5 as a function of α. It can be seen that the activation energy is practically independent of the value of α for the data obtained by the DSC instruments (*A*, *B*, *D* and *E*). Nevertheless, it depends strongly on α for DTA instrument *C*. This effect is probably caused by thermal inertia phenomena. Hence, from this point of view, the DTA method is not very appropriate for kinetic analyses.

Table 5 summarizes average values of the activation energy calculated by the Friedman, Ozawa and Kissinger methods. These values are in reasonable agreement for the instruments *B*, *D* and *E* but differ substantially (by

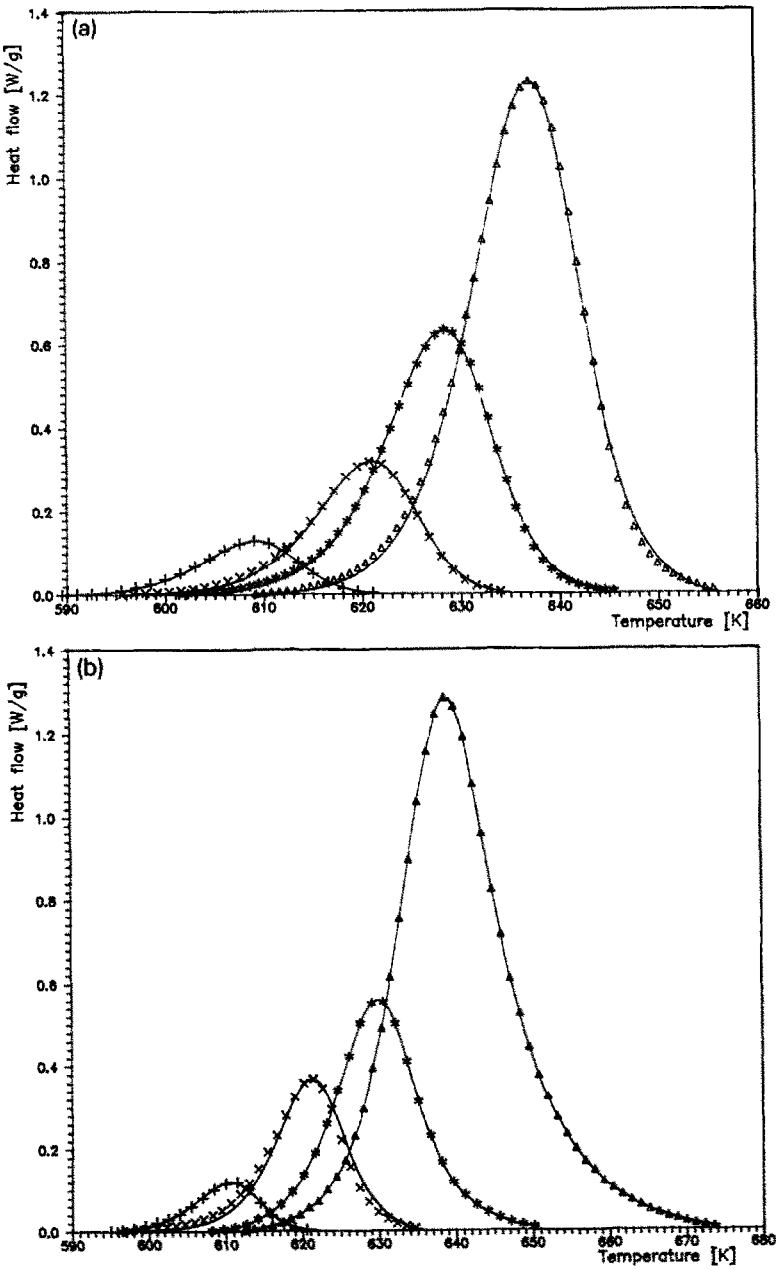

Fig. 4. Experimental (points) and calculated crystallization peaks (full lines) for the instrument (a) A and (b) C. The heating rates are shown by various points, i.e. (+), 2, (×) 5, (*) 10 and (△) 20 K min^{-1}.

about 20%) for instruments A and C. This difference can be explained by the different thermal pre-treatment of the glassy sample [21]. In this case the sample was rapidly heated in the DSC holder up to 523 K (above T_g) at a

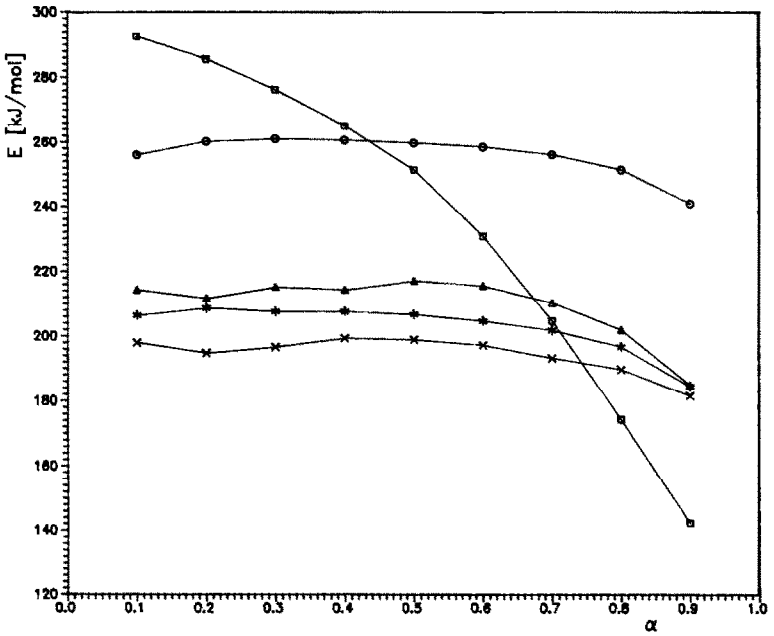

Fig. 5. Activation energies at various values of α calculated by the Friedman method for the instruments: (○) *A*, (△) *B*, (□) *C*, (×) *D* and (*) *E*.

heating rate of 320 K min^{-1}, and after 3 min the DSC scan was started using the selected heating rate.

Figures 6 and 7 show the $y(\alpha)$ and $z(\alpha)$ dependences for kinetic data obtained by instruments *A* and *C*. These dependences were calculated using eqns. (6) and (4) for the values of the activation energy calculated by the Kissinger method. If the kinetic behavior is the same, the experimentally determined $y(\alpha)$ and $z(\alpha)$ functions have to be independent of heating rate. Although there is a certain degree of dispersion of the points corresponding to instrument *A* in Figs. 6 and 7, the overall pattern is sufficient to justify the above assumption, at least for $\beta \leq 20$ K min^{-1}. On the other hand, the

TABLE 5

The values of *E* (kJ mol^{-1})

Instrument	Method		
	Friedman	Ozawa	Kissinger
A	256± 9	249±11	251±10
B	209± 6	218± 4	215± 4
C	236±41	254±11	256±10
D	194±18	211±24	214±18
E	203±15	205±12	204±15

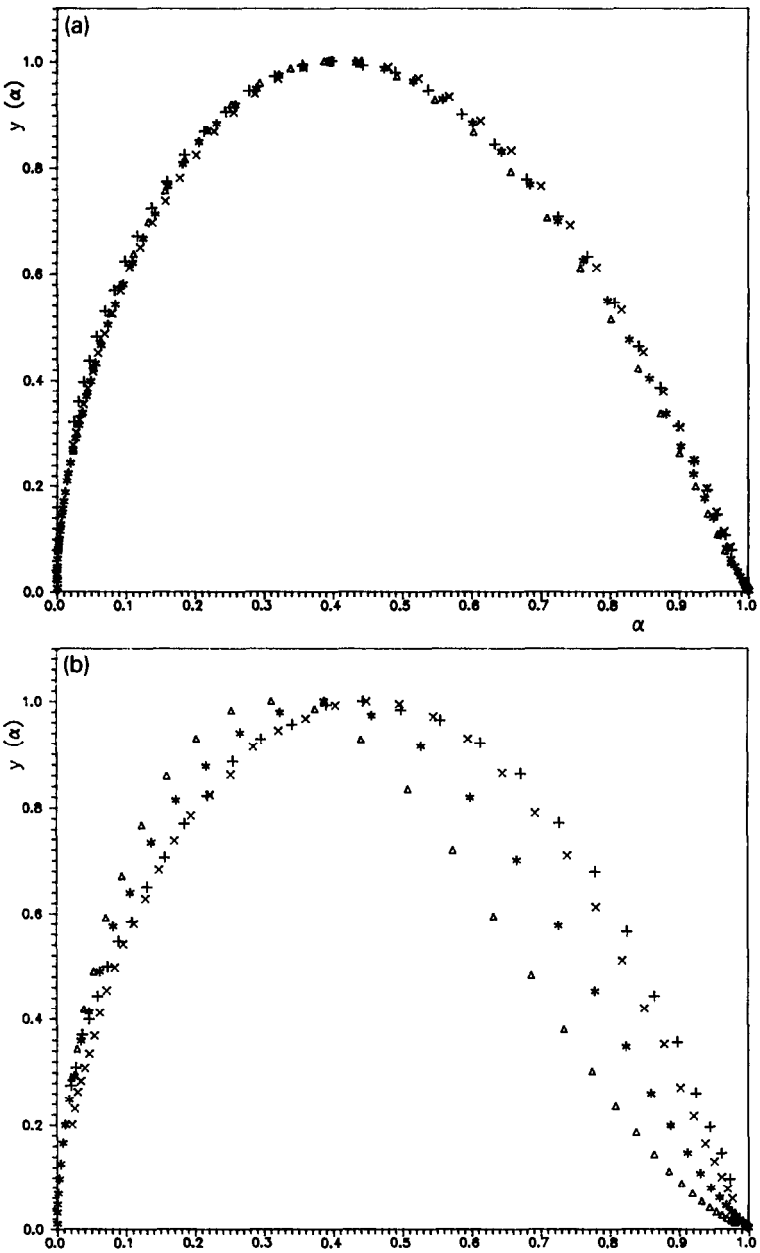

Fig. 6. Normalized $y(\alpha)$ functions corresponding to the crystallization kinetic data measured by the instruments (a) A and (b) C at various heating rates. The meaning of the symbols is as in Fig. 4.

$y(\alpha)$ and $z(\alpha)$ functions for instrument C vary considerably with β, especially for higher heating rates. This behavior can be explained by thermal inertia effects and because the DTA device cannot maintain a

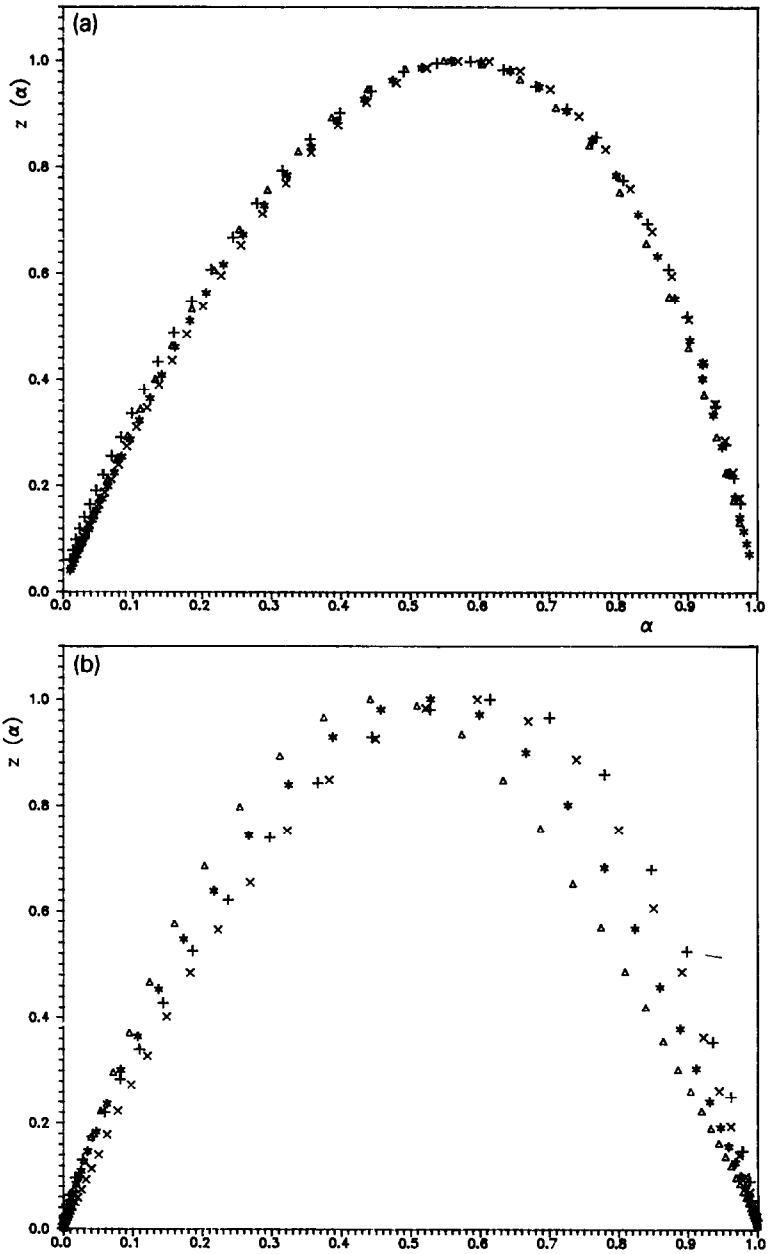

Fig. 7. Normalized $z(\alpha)$ functions corresponding to the crystallization kinetic data measured by instruments (a) *A* and (b) *C* at various heating rates. The meaning of the symbols is as in Fig. 4.

controlled heating rate during the crystallization process, which is inherent to the DTA method.

The values of α_m and α_p^∞ corresponding to the maxima of both $y(\alpha)$ and

TABLE 6

The values of α_m and α_p^∞

Instrument	α_m	α_p^∞
A	0.41±0.01	0.57±0.01
B	0.43±0.03	0.56±0.01
C	0.39±0.06	0.54±0.06
D	0.40±0.01	0.57±0.02
E	0.44±0.01	0.57±0.01

TABLE 7

The kinetic parameters for data taken with instrument *A*

β (K min^{-1})	*m*	*n*	ln *A* (s^{-1})	ΔH_c (J g^{-1})
2	0.642	0.940	44.78	48.77
5	0.712	0.947	44.79	49.10
10	0.689	1.023	44.77	57.73
20	0.710	1.074	44.87	55.05

TABLE 8

The kinetic parameters for data taken with instrument *B*

β (K min^{-1})	*m*	*n*	ln *A* (s^{-1})	ΔH_c (J g^{-1})
2.5	0.526	0.831	37.56	50.43
5	0.573	0.902	37.74	52.87
10	0.810	0.960	38.00	44.24
20	0.787	1.089	37.72	63.11

TABLE 9

The kinetic parameters for data taken with instrument *C*

β (K min^{-1})	*m*	*n*	ln *A* (s^{-1})	ΔH_c (J g^{-1})
2	0.673	0.890	45.60	45.73
5	0.862	1.003	46.00	49.11
10	0.828	1.346	45.88	67.47
20	0.728	1.603	45.76	67.47

TABLE 10

The kinetic parameters for data taken with instrument *D*

β (K min^{-1})	*m*	*n*	ln *A* (s^{-1})	ΔH_c (J g^{-1})
2	0.539	0.859	37.42	57.59
5	0.638	0.899	37.49	59.57
10	0.711	0.972	37.79	49.51
20	0.651	1.032	37.53	52.12

$z(\alpha)$ curves are summarized for all instruments in Table 6. It is evident that the values of these important parameters conform to the SB(m, n) model. The kinetic parameters for this model calculated by eqns. (10)–(13) are shown in Tables 7–11. As has been mentioned above, the kinetic parameters for the data measured by instruments A and C differ because of different thermal treatments of the sample and due to instrumental factors. Therefore, there are only three sets of the kinetic parameters corresponding to the experiments carried out at the same conditions (see B, D, E in Tables 8, 10 and 11). Taking these values we can calculate average kinetic parameters for the crystallization of the Sb_2S_3 compound in $(GeS_2)_{0.3}(Sb_2S_3)_{0.7}$ glass as follows: $E = 211 \pm 6$ kJ mol^{-1}, $m = 0.68 \pm 0.09$, $n = 0.94 \pm 0.08$ and ln $A = 37 \pm 1$ s^{-1}. There is also relatively good agreement between both the measured and the calculated values of the reaction heat, i.e. $\Delta H_e = 52 \pm 1$ J g^{-1} and $\Delta H_c = 54 \pm 6$ J g^{-1}.

Ryšavá and co-workers [22–24] have suggested that the crystallization of the bulk $(GeS_2)_{0.3}(Sb_2S_3)_{0.7}$ glass can be interpreted in terms of the JMA(n) model, and reported the values of kinetic parameters $n = 1.9$ and $E = 159$–178 kJ mol^{-1} determined by both the isothermal and the non-isothermal method. In this case the parameter α_p^∞ should be 0.633 (see Section 2.4). Nevertheless, we observed a considerably lower value of this parameter and therefore it is difficult to obtain a good agreement of the experimental data and calculated DSC curves for the JMA(n) model. This is evident in Fig. 8, where the calculated DSC curves corresponding to both the SB(m, n) and the JMA(n) model are compared with theoretical data measured with the instrument E. The average kinetic parameters calculated using eqns. (8), (9), (12) and (13) for the JMA(n) model can be summarized as follows: $n = 2.0 \pm 0.3$, ln $A = 36 \pm 1$ s^{-1} and $\Delta H_c = 52 \pm 11$ J g^{-1}. The value of the activation energy is the same as for the SB(m, n) model because it is invariant with respect to the kinetic model. This value is higher than that published for the bulk sample (see above). A similar difference was also observed for Ge_xS_{1-x} glasses, and can be explained by the fact that in the two cases (bulk and powder sample) the crystals of Sb_2S_3 grow from a different number of nuclei [25].

It is without any doubt that the formal Šesták–Berggren model allows more quantitative description of the studied process than other models.

TABLE 11

The kinetic parameters for data taken with instrument E

β (K min^{-1})	m	n	ln A (s^{-1})	ΔH_c (J g^{-1})
2.5	0.642	0.823	35.26	56.95
5	0.731	0.939	35.31	57.48
10	0.737	0.910	35.58	57.45
20	0.791	1.032	35.50	57.45

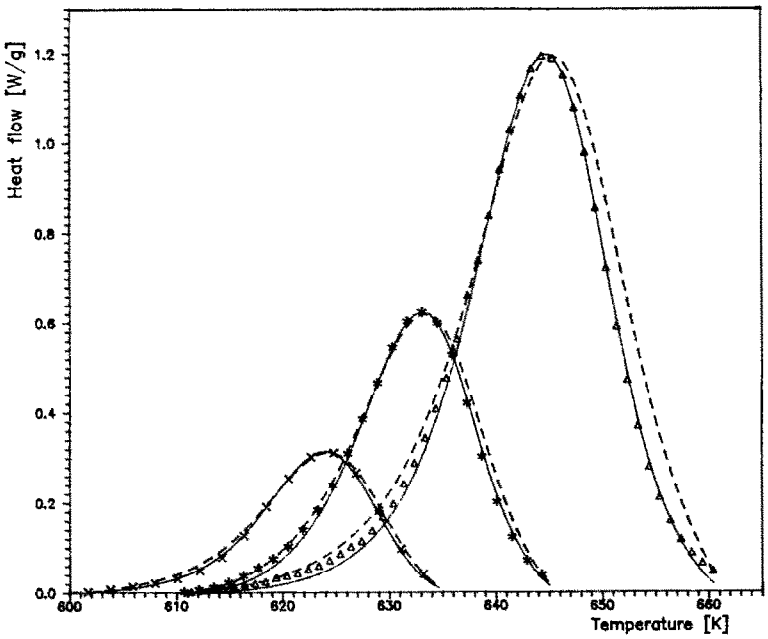

Fig. 8. Experimental (points) DSC crystallization data measured by instrument E for three different heating rates. Calculated curves corresponding to the SB(m, n) and JMA(n) model are shown by full and dashed lines, respectively. The meaning of the symbols is as in Fig. 4.

Similar results were published for the crystallization of Bi_2S_3 in $(GeS_2)_{0.5}(Bi_2S_3)_{0.5}$ glass [26] and for crystallization of both GeS and GeS_2 in the Ge_xS_{1-x} glass system [27–29]. Nevertheless, it should be pointed out that the kinetic parameters calculated cannot say anything definitive about the real mechanism of the crystallization process. From this point of view, attention should be drawn to morphological investigations [4].

CONCLUSIONS

It was found that it is impossible to make a reliable kinetic analysis using only one non-isothermal crystallization curve. However, several measurements at various heating rates provide determination of the activation energy and thus enable us to get some insight as to which is the most convenient kinetic model of the crystallization process. A simple method of kinetic analysis has been developed and applied to the study of crystallization of the Sb_2S_3 phase in $(GeS_2)_{0.3}(Sb_2S_3)_{0.7}$ glass measured by various DSC and DTA instruments. It was established that this crystallization process can be described by the Šesták–Berggren model. It seems that the JMA(n) model is not suitable for a quantitative description of this process.

ACKNOWLEDGEMENTS

The authors are indebted to Dr. N. Ryšavá and Dr. V. Špaček for their help with the measurements with the Du Pont 990 and Perkin–Elmer DSC-2 instruments, respectively.

REFERENCES

1 K. Matusita and S. Sakka, Phys. Chem. Glasses, 20 (1979) 81.
2 D.W. Henderson, J. Non-Cryst. Solids, 30 (1979) 301.
3 S. Suriñach, M.D. Baró, M.T. Clavaguera-Mora and N. Clavaguera, J. Non-Cryst. Solids, 58 (1983) 209.
4 D.W. Henderson and D.G. Ast, J. Non-Cryst. Solids, 64 (1984) 43.
5 H. Yinnon and B.R. Uhlmann, J. Non-Cryst. Solids, 50 (1982) 189.
6 J. Šesták, Thermophysical Properties of Solids, Their Measurement and Theoretical Analysis, Elsevier, Amsterdam, 1984.
7 G.I. Senum and R.T. Yang, J. Therm. Anal., 11 (1977) 445.
8 H.E. Kissinger, Anal. Chem., 29 (1957) 1702.
9 T. Ozawa, J. Therm. Anal., 2 (1979) 301.
10 H.L. Friedman, J. Polym. Sci., Part C, C6 (1964) 183.
11 J.M. Criado, J. Málek and A. Ortega, Thermochim. Acta, 147 (1989) 337.
12 J. Málek, Thermochim. Acta, 138 (1989) 337.
13 J. Málek and J.M. Criado, Thermochim. Acta, 175 (1991) 305.
14 J. Málek, J.M. Criado, J. Šesták and J. Militký, Thermochim. Acta, 153 (1989) 429.
15 E.S. Freeman and B. Carroll, J. Phys. Chem., 62 (1958) 394.
16 J.M. Criado, D. Dollimore and G.R. Heal, Thermochim. Acta, 54 (1982) 159.
17 V.M. Gorbachev, J. Therm. Anal., 27 (1983) 151.
18 V. Šatava, Thermochim. Acta, 2 (1971) 423.
19 J. Málek and J.M. Criado, Thermochim. Acta, 164 (1990) 199.
20 C.M. Earnest, Thermal Analysis of Clays, Minerals and Coal, Perkin–Elmer, Norwalk, CT, 1984.
21 A. Marotta, A. Buri and F. Branda, J. Mater. Sci., 16 (1981) 341.
22 N. Ryšavá, L. Tichý, C. Barta, A. Tříska and H. Tichá, Phys. Status Solidi A, 87 (1985) K13.
23 N. Ryšavá, T. Spasov and L. Tichý, J. Therm. Anal., 32 (1987) 1015.
24 N. Ryšavá, C. Barta and L. Tichý, J. Mater. Sci. Lett., 8 (1989) 91.
25 A. Marotta, A. Buri and F. Branda, Thermochim. Acta, 40 (1980) 397.
26 L. Tichy and P. Nagels, Phys. Status Solidi A, 107 (1988) 769.
27 J. Málek and J. Klikorka, J. Therm. Anal., 32 (1987) 1883.
28 J. Málek, Thermochim. Acta, 129 (1988) 293.
29 J. Málek, J. Non-Cryst. Solids, 107 (1989) 323.